

ARTICLE

Received 23 Apr 2014 | Accepted 29 Sep 2014 | Published 14 Nov 2014

DOI: 10.1038/ncomms6410

Decreased tumorigenesis in mice with a *Kras* point mutation at C118

Lu Huang¹, John Carney², Diana M. Cardona² & Christopher M. Counter^{1,3}

KRAS, *NRAS* or *HRAS* genes are mutated to encode an active oncogenic protein in a quarter of human cancers. Redox-dependent reactions can also lead to Ras activation in a manner dependent upon the thiol residue of cysteine 118 (C118). Here, to investigate the effect of mutating this residue on tumorigenesis, we introduce a C118S mutation into the endogenous murine *Kras* allele and expose the resultant mice to the carcinogen urethane, which induces *Kras* mutation-positive lung tumours. We report that *Kras*^{+/C118S} and *Kras*^{C118S/C118S} mice develop fewer lung tumours. Although the *Kras*^{C118S} allele does not appear to affect tumorigenesis when the remaining *Kras* allele is conditionally oncogenic, there is a moderate imbalance of oncogenic mutations favouring the native *Kras* allele in tumours from *Kras*^{+/C118S} mice treated with urethane. We conclude that the *Kras*^{C118S} allele impedes urethane-induced lung tumorigenesis.

¹Department of Pharmacology and Cancer Biology, Duke University Medical Center, Durham, North Carolina 27710, USA. ²Department of Pathology, Duke University Medical Center, Durham, North Carolina 27710, USA. ³Department of Radiation Oncology, Duke University Medical Center, Durham, North Carolina 27710, USA. Correspondence and requests for materials should be addressed to C.M.C. (email: count004@mc.duke.edu).

The Ras family of small GTPases, comprised of the *KRAS*, *NRAS* and *HRAS* genes, are mutated to encode constitutively active, GTP-bound, oncogenic proteins in upwards of one quarter of all human cancers, which is well established to promote tumorigenesis¹. Despite the prominent role these genes play in human cancer, the encoded proteins have proven difficult to pharmacologically inhibit^{2,3}. As such, it is important to understand how Ras proteins are activated. In this regard, Ras proteins cycle between GDP-bound inactive and GTP-bound active states, the latter being catalysed by guanine nucleotide exchange factors (GEFs)^{4,5}. GEFs are not, however, the only means of activating Ras proteins. Free radical oxidants can lead to S-nitrosylation or S-glutathiolation and activation of Ras in a manner dependent on the thiol residue of cysteine 118 (C118)^{6–8}. Accumulating evidence supports the possibility that such redox-dependent reactions with C118 may have cellular consequences. Specifically, an increase in S-nitrosylation and activation of Ras can stimulate MAP-kinase (MAPK) signalling^{6,9–14}, phosphatidylinositol 3-kinase signalling¹⁵ and/or cell proliferation¹⁶. Similarly, an increase in S-glutathiolation and activation of Ras impacts a variety of signalling pathways in a manner apparently dependent upon C118 (refs 17,18). Finally, reducing the expression of endothelial nitric oxide synthase (eNOS), which catalyses the production of nitric oxide¹⁹, decreases the levels of S-nitrosylated and active Ras as well as xenograft tumour growth in a number of cancer cell lines²⁰.

Despite accumulating data, the effect of specifically blocking redox-dependent reactions with C118 on the function of endogenous mammalian Ras remains to be explored *in vivo*. This is especially important in terms of cancer, as tumour initiation appears to be sensitive to the level of activated Ras²¹. Fortunately, there is a very precise separation-of-function mutation that apportions these effects from other functions of Ras. Specifically, substitution of C118 for serine (C118S), a very minor modification in which the thiol residue of this cysteine is replaced with a hydroxyl group, renders Ras completely insensitive to activation by free radical-mediated oxidants, with no measurable effect on the protein structure, GTPase activity, intrinsic and GEF-mediated guanine nucleotide dissociation rate, or the ability to bind an effector^{6,8,10,12,17,18,22–24}. Thus, here we assess the consequences of introducing the C118S mutation into the endogenous murine *Kras* gene on tumorigenesis *in vivo*, and find a reduction in carcinogen-induced lung tumorigenesis in mice bearing this mutated allele.

Results

Generation of mice with a *Kras*^{C118S} allele. To investigate the effect of mutating C118 on Ras function *in vivo* during tumorigenesis, a targeting vector was created to insert a single-point mutation, namely a G353 transversion to C (G353 > C) encoding the C118S mutation, into exon 3 of the murine *Kras* gene (Fig. 1a). C118S was chosen because this precise separation-of-function mutation specifically blocks the redox-dependent reactions at this site that lead to Ras activation^{6,8,10,12,17,18,22–24}. *Kras* was chosen, as this is the isoform most commonly mutated in human cancers¹. This vector was electroporated into embryo stem (ES) cells, and cells were selected for resistance to G418 and ganciclovir. Successful recombination events in resistant clones were verified by reverse transcription (RT)-PCR and sequencing to contain the G353 > C transversion in *Kras* (Fig. 1b). One such clone was used to generate a founder *Kras*^{+ / C118S(Neo)} mouse, the genotype of which was identified by PCR amplification from genomic DNA. A 314-bp product unique to the targeted *Kras*^{C118S(Neo)} allele was amplified (Supplementary Fig. 1a) using primers anchored in exon 3 of the *Kras* gene and in the

Neo gene of the targeting vector (P3 and P4, Fig. 1a and Supplementary Table 4), whereas a 621-bp product unique to the wild-type *Kras* allele was amplified (Supplementary Fig. 1a) using primers anchored in exon 3 and in the adjacent intron (P3 and P5, Fig. 1a and Supplementary Table 4). These mice were crossed with *CMVCre* transgenic mice to induce Cre-mediated recombination between the *loxP* sites flanking the *Neo* cassette. Successful excision of the *Neo* cassette was identified by PCR amplification of genomic DNA, yielding a 517-bp, instead of a 621-bp product, using primers P3 and P5, as well as by confirming the absence of the aforementioned 314bp product using primers P3 and P4 (Supplementary Fig. 1b). The presence of *CMVCre* was identified by PCR amplification of genomic DNA using primers (P16 and P17, Supplementary Table 4) designed to generate a 100-bp PCR product unique to this transgene (Supplementary Fig. 1b). *CMVCre;Kras*^{+ / C118S} mice identified in this manner were then crossed with *Kras*^{+ / +} mice to generate *Kras*^{+ / C118S} mice without *CMVCre* for use in subsequent experiments, again with the desired genotypes confirmed by similar PCR strategies. Finally, *Kras*^{+ / C118S} mice were crossed, generating *Kras*^{+ / +}, *Kras*^{+ / C118S} and *Kras*^{C118S / C118S} offspring, the genotype of which were identified by PCR amplification of genomic DNA using the aforementioned primer pair P3 and P5 (Fig. 1a and Supplementary Table 4) that distinguished wild-type versus C118S *Kras* alleles by the amplification of a 621-bp versus a 517-bp product (Fig. 1c and Supplementary Fig. 6a).

Characterization of the *Kras*^{C118S} allele. We confirmed that the strategy to introduce the G353 > C transversion into the *Kras* gene did not overtly affect alternative splicing of terminal exons 4A and 4B, an important consideration as both splice forms are important for carcinogen-induced lung tumorigenesis^{25,26}. Specifically, RT-PCR analysis with primers designed to amplify only *Kras* 4A or only *Kras* 4B detected both versions in lung tissue isolated from *Kras*^{+ / +} and *Kras*^{C118S / C118S} mice (Fig. 1d and Supplementary Fig. 6b). Similarly, we confirmed that this alteration of the *Kras* gene did not overtly affect protein expression, given that tumour initiation is sensitive to the level of Ras protein²¹. Specifically, immunoblot analysis revealed no detectable difference in the amount of *Kras* protein in lung tissue isolated from *Kras*^{+ / +} versus *Kras*^{C118S / C118S} mice (Fig. 1e and Supplementary Figs 2 and 6c). Finally, we demonstrate that introducing the C118S mutation into endogenous *Kras* gene can affect the ability of eNOS to stimulate the MAPK pathway. Specifically, mouse embryonic fibroblasts (MEFs) were isolated from two control *Kras*^{+ / +} and two experimental *Kras*^{C118S / C118S} embryos and immortalized with the SV40 early region. These four cell lines were then stably infected with a retrovirus encoding no transgene or the S1177D-activated mutant version of HA-tagged eNOS^{27,28}. Lysates isolated seven independent times from the resultant eight cell lines were then immunoblotted for ectopic eNOS, endogenous *Kras* and tubulin, as well as total (T) and phosphorylated (P) Erk1/2. Although the normalized levels of P-Erk1/2 varied from experiment to experiment among the samples, on average there was a smaller fold increase in the normalized P-Erk1/2 levels upon expression of eNOS^{S1177D} in *Kras*^{C118S / C118S} compared with *Kras*^{+ / +} MEFs (0.90 ± 0.14 versus 3.21 ± 0.91, *P* < 0.02, Fig. 2 and Supplementary Fig. 6d). Collectively, we conclude that the single G353 > C transversion encoding the desired C118S mutation was successfully knocked into the *Kras* locus with no overt effect on the expression of the resultant gene products.

***Kras*^{C118S / C118S} mice appear normal.** Identification of genotypes of 580 offspring from crossing *Kras*^{+ / C118S} mice revealed that

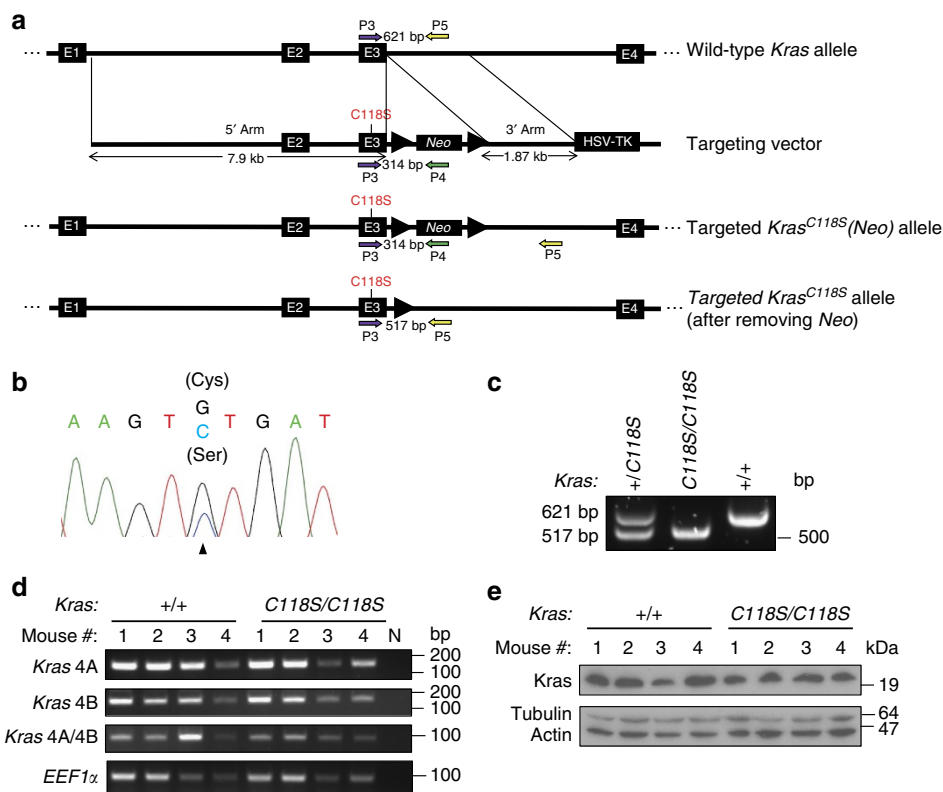


Figure 1 | Generation of mice with a *Kras*^{C118S} allele. (a) Schematic representation of homologous recombination (thin black lines) between the endogenous wild-type *Kras* gene (E-numbered black boxes: exons, thick black lines: introns) and the *Kras*^{C118S}-targeting vector (*Neo*: Neo selection marker; thick arrows: *loxP* recombination sites; HSV-TK: HSV promoter-driven thymidine kinase-negative selection marker) as well as the resultant targeted *Kras*^{C118S} knock-in allele before and after Cre-mediated recombination of the flanking *loxP* sites to excise the *Neo* selection marker. Coloured arrows: PCR primers used in genotyping. (b) Sequencing chromatogram of RT-PCR amplified *Kras* mRNA from a successfully targeted ES cell clone identifying the wild-type (G) and mutated (C) nucleotide at position 353 that changes the cysteine 118 to serine. (c) PCR amplification using the primer pair P3 + P5 of genomic DNA from offspring of the indicated genotypes from crossing *Kras*^{+/C118S} mice. (d) RT-PCR amplification of *Kras* mRNA from the lungs of four *Kras*^{+/+} mice and four *Kras*^{C118S/C118S} mice (numbered 1, 2, 3 and 4) using primer pairs specific for the indicated *Kras* splice variants (see Supplementary Table 4). N: no DNA as a negative control reaction. *EEF1α*: loading control. (e) Immunoblot of lysates isolated from the lungs of four *Kras*^{+/+} mice and four *Kras*^{C118S/C118S} mice (numbered 1, 2, 3 and 4) with an anti-*Kras* antibody. Tubulin and actin: loading controls.

there was no statistical difference between the observed frequency versus the expected Mendelian ratio of the three genotypes of *Kras*^{+/+}, *Kras*^{+/C118S} and *Kras*^{C118S/C118S} (χ^2 test, $P=0.545$, Table 1). *Kras*^{C118S/C118S} mice were also phenotypically indistinguishable from *Kras*^{+/+} mice (Fig. 3a). Weekly weight measurements, beginning at 8 weeks of age and continuing for another 17 weeks, revealed no statistical difference in the weight of either male or female mice between the *Kras*^{+/+} versus *Kras*^{C118S/C118S} genotypes (Fig. 3b,c). The *Kras*^{-/-} genotype is embryonic to neonatal lethal, and is characterized by defective cardiovascular function²⁹. As heart defects are a hallmark of defective *Kras* function, we also compared the heart-to-body weight ratio between *Kras*^{+/+} versus *Kras*^{C118S/C118S} mice, finding no significant difference between the two cohorts (Fig. 3d). Finally, *Kras*^{+/+} mice had a median lifespan of 847 days, whereas *Kras*^{C118S/C118S} mice had a median lifespan of 670 days, but the difference was not significant (Fig. 3e). Collectively, these data indicate that mice with one or more *Kras*^{C118S} alleles do not have any obvious developmental or physiological defects.

Reduced carcinogenesis in mice with a *Kras*^{C118S} allele. To determine the impact of the *Kras*^{C118S} mutation on carcinogenesis, we assessed the effect of treating *Kras*^{+/+}, *Kras*^{+/C118S} and *Kras*^{C118S/C118S} mice with the carcinogen urethane (ethyl

carbamate), which induces lung tumours characterized by oncogenic Q61R/L mutations in *Kras*³⁰. We chose this approach to model a *Kras* mutation-positive cancer spontaneously arising from an environmental insult³⁰ in the lung, especially given the prevalence of *KRAS* mutations in human lung cancer³¹. As an important note, the *Pas1* locus responsible for the different susceptibilities to urethane-induced tumorigenesis observed among inbred strains of mice maps to a region containing six genes, one being *Kras*³². Therefore, *Kras*^{+/C118S} mice, which possess the *Kras*^{C118S} allele from the 129S6/SvEvTac background, but the other native *Kras* allele from the C57/BL6 background (introduced during the excision of the *Neo* cassette), were crossed with *Kras*^{+/+} mice from the 129S6/SvEvTac background. Resultant *Kras*^{+/C118S} mice were then crossed to generate *Kras*^{+/+}, *Kras*^{+/C118S} and *Kras*^{C118S/C118S} mice in which both *Kras* alleles originated from a 129S6/SvEvTac background. Cohorts of 27 *Kras*^{+/+}, 25 *Kras*^{+/C118S} and 25 *Kras*^{C118S/C118S} littermates from multiple breeding pairs were then intraperitoneally injected with urethane at 8 weeks of age. Eight months later, mice from all three cohorts were euthanized and lungs removed for analysis.

Comparison of the number and size of visible surface lung lesions revealed that *Kras*^{+/C118S} and *Kras*^{C118S/C118S} mice developed fewer tumours with a smaller average tumour size, resulting in an overall reduction in tumour burden, as defined by

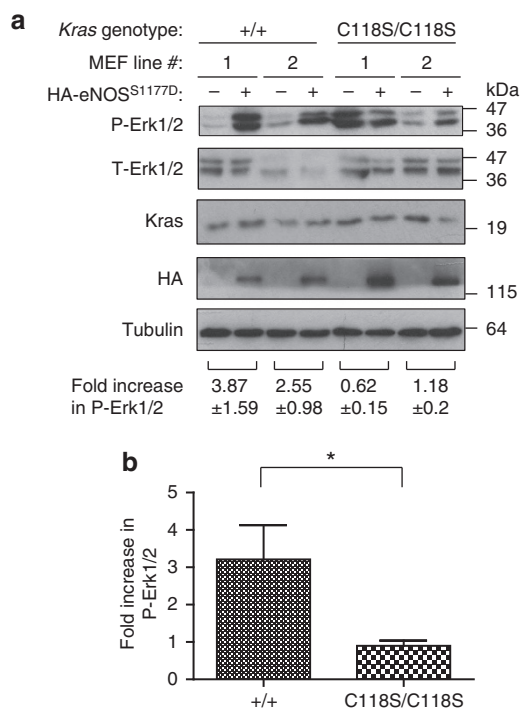


Figure 2 | Reduced increase in P-Erk1/2 levels in *Kras*^{C118S/C118S} MEFs upon expressing activated eNOS. (a) Immunoblot of HA-tagged ectopic eNOS, endogenous Kras and tubulin, as well as total (T) and phosphorylated (P) Erk1/2 from two *Kras*^{+/+} and two *Kras*^{C118S/C118S} SV40-immortalized MEF cell lines in the absence or presence of HA-eNOS^{S1177D}. Bottom: mean ± s.e.m. of the indicated fold increase in P-Erk1/2 (normalized to T-Erk1/2) from immunoblot analysis of lysates derived seven independent times. **(b)** Mean ± s.e.m. fold increase in P-Erk1/2 levels (normalized to T-Erk1/2) upon expression of eNOS^{S1177D} from lysates derived seven independent times from the two *Kras*^{+/+} (+/+) or two *Kras*^{C118S/C118S} (C118S/C118S) SV40-immortalized MEF cell lines. **P* < 0.05, as determined by two-tailed unpaired Student's *t*-test.

the sum of the diameters of all visible surface tumours per mouse, compared with control *Kras*^{+/+} mice. There was no statistical difference in tumour number or size between the *Kras*^{+/C118S} and *Kras*^{C118S/C118S} cohorts (Fig. 4a–d and Table 2). Binning tumours based on size, namely small (≤ 1 mm), medium (1–3 mm) or large (≥ 3 mm), revealed a significant shift (χ^2 test, *P* = 0.0014) from larger tumours in *Kras*^{+/+} mice to smaller tumours in *Kras*^{C118S/C118S} mice (Table 2). To independently validate these results, one lung from each of the mice in the three cohorts was formalin fixed, paraffin embedded, sectioned, haematoxylin and eosin (H&E)-stained, and the type and size of tumours analysed. Focusing on the most common type of lesion, adenomas were microscopically counted and binned as above as being small, medium or large. Again, there was a shift to smaller tumours in mice having one or more *Kras*^{C118S} alleles. Specifically, large adenomas were only detected in *Kras*^{+/+} mice, and these mice also had a higher incidence of adenomas of medium size, whereas *Kras*^{+/C118S} and *Kras*^{C118S/C118S} mice had a statistically higher incidence of small-sized adenomas (χ^2 test, *P* ≤ 0.01 , Table 3). Collectively, these data demonstrate that the presence of the *Kras*^{C118S} allele impairs urethane carcinogenesis.

To assess whether there was also an impact on tumour progression, lesions were graded³³ as being atypical adenomatous hyperplasia (AAH), adenoma (AD), or adenocarcinoma (AC) by histology (Supplementary Fig. 3). This analysis revealed a similar tumour spectrum among the three genotypes. Specifically,

Table 1 | Expected and observed frequencies of offspring from crossing *Kras*^{+/C118S} mice.

<i>Kras</i> genotype	Expected frequency	Observed frequency
+/+	25% (145/580)	26.72% (155/580)
+/C118S	50% (290/580)	47.93% (278/580)
C118S/C118S	25% (145/580)	25.34% (147/580)

regardless of the genotype, the majority of the tumours were AD, with only a few AAH and an infrequent number of AC in each group (Supplementary Table 1). AD lesions were further classified³⁴ into papillary, solid or mixed solid/papillary subtypes (Supplementary Fig. 3). There was no significant difference in the incidence of solid AD among the three groups, although the *Kras*^{+/C118S} mice appeared to have fewer papillary AD and more mixed solid/papillary AD (Supplementary Table 2). Finally, immunohistochemical analysis of lung lesions in four to six random microscope fields from five mice each having the genotypes *Kras*^{+/+}, *Kras*^{+/C118S} or *Kras*^{C118S/C118S} after treatment with urethane did not show any overt difference in the level of Ras signalling, as assessed by P-Erk1/2 or P-Akt immunostaining, or in proliferation, as assessed by Ki67 immunostaining, with the exception of reduced P-Akt in the *Kras*^{+/C118S} cohort (Supplementary Fig. 4a,b). Collectively, these data point towards a negative effect of the *Kras*^{C118S} allele, particularly at the stage of tumour initiation.

Similar tumorigenesis between *Kras*^{LSL-G12D/+} and *Kras*^{LSL-G12D/C118S} mice. In the urethane-induced lung tumour model, typically only one *Kras* allele acquires an oncogenic mutation. Although the oncogenic *Kras* allele is well established to promote tumorigenesis, the remaining non-oncogenic allele has actually been found to be tumour suppressive in some settings³⁵. As such, the observed negative effect of the *Kras*^{C118S} allele on lung tumorigenesis is ostensibly due to the C118S mutation either suppressing the tumorigenic activity of oncogenic *Kras* allele and/or enhancing tumour suppressive effect of the remaining non-oncogenic *Kras* allele. To test the latter possibility, we took advantage of mice with a conditionally oncogenic *LSL-Kras*^{G12D} allele to compare the effect of the remaining *Kras* allele with or without a C118S mutation on lung tumorigenesis. In more detail, infection of lung tissue upon intranasal administration of adenovirus encoding Cre (AdCre) induces recombination of *loxP* sites flanking a transcriptional/translational STOP sequence (*LSL*) upstream of *Kras* harbouring a G12D oncogenic mutation, thereby permitting expression of the *Kras*^{G12D} allele, which promotes lung tumorigenesis³⁶. Thus, *LSL-Kras*^{G12D/+} mice were crossed with *Kras*^{+/C118S} mice in which both *Kras* alleles were of the 129S6/SvEvTac background. Cohorts of 21 resultant *Kras*^{LSL-G12D/+} and 17 *Kras*^{LSL-G12D/C118S} littermates from multiple breeding pairs were treated intranasally with AdCre at 8 weeks of age. Four months later mice from both cohorts were euthanized and lungs removed for analysis. Quantification of the number, size and total burden of visible surface lesions revealed no statistical difference between the two cohorts (Fig. 5a–c). The sizes of these cohorts are powered to detect differences in the number, burden and size of 1.52, 1.78 and 0.52 mm, respectively. Similarly, microscopic quantification of the number of lesions in H&E-stained lung sections from these mice (Supplementary Fig. 5) revealed no significant difference between these two cohorts (Fig. 5d). Thus, the *Kras*^{C118S} allele does not appear to confer any overt change to the tumour-suppressive activity to the non-oncogenic allele in a lung tumour model driven by *Kras*^{G12D}.

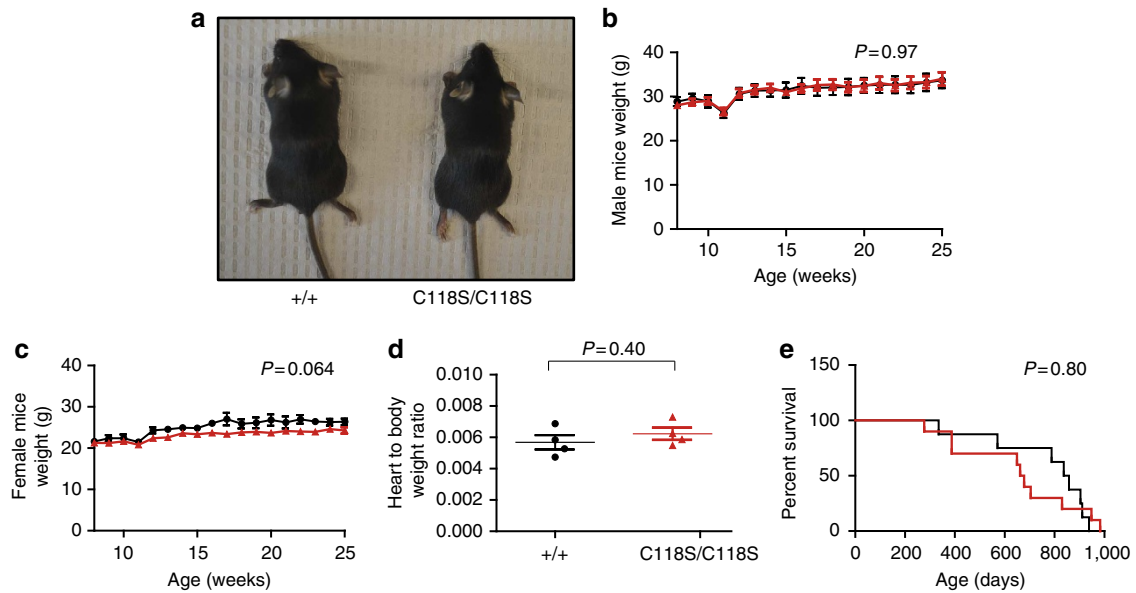


Figure 3 | *Kras*^{C118S/C118S} mice have no overt phenotypes. (a) Photograph of a *Kras*^{+/+} (+/+) and *Kras*^{C118S/C118S} (C118S/C118S) adult mouse at 3 weeks of age. (b,c) Mean body weight ± s.e.m. of (●) *Kras*^{+/+} versus (▲) *Kras*^{C118S/C118S} (b) male (n=6 versus 5) and (c) female mice (n=4 versus 5) from 8 to 25 weeks of age. (d) Mean heart to body weight ratio ± s.e.m. of 4-week-old *Kras*^{+/+} (+/+) versus *Kras*^{C118S/C118S} (C118S/C118S) mice (n=4). (e) Kaplan-Meier survival curves of *Kras*^{+/+} (black line, n=8) versus *Kras*^{C118S/C118S} (red line, n=10) mice. P value was determined by multivariate analysis of variance test (b,c), two-tailed unpaired Student's t-test (d) and long-rank test (e).

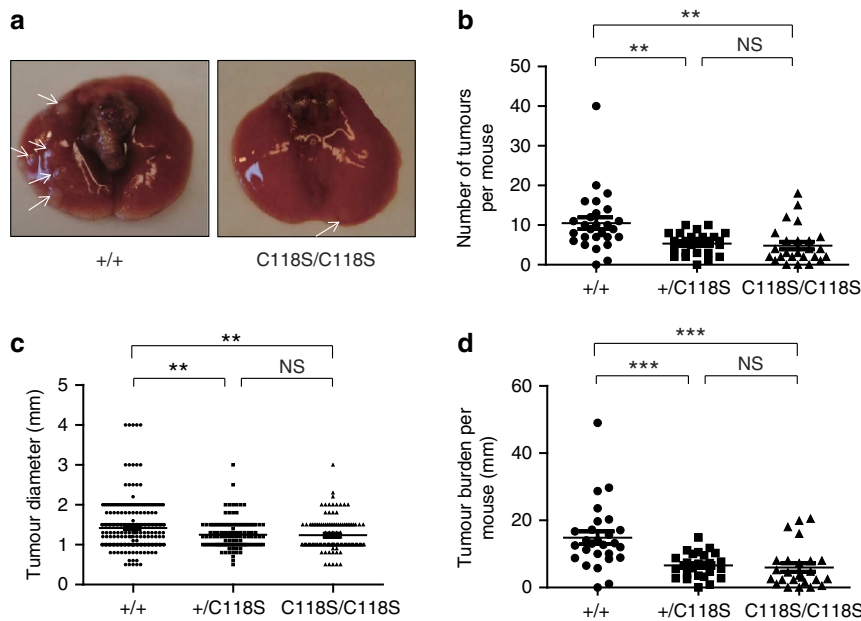


Figure 4 | Decreased urethane-induced lung tumorigenesis in mice with a *Kras*^{C118S} allele. (a) Visible lesions (arrows) of lungs from one *Kras*^{+/+} (+/+) and one *Kras*^{C118S/C118S} (C118S/C118S) mouse 8 months after treatment with urethane. (b) Number of visible surface tumour lesions per mouse, (c) diameter of each visible surface tumour lesion and, (d) tumour burden, as defined by the sum of the diameters of all visible surface tumour lesions per mouse, from *Kras*^{+/+} (+/+, 27 mice, 285 visible surface tumours), *Kras*^{+/C118S} (+/C118S, 25 mice, 132 visible surface tumours) and *Kras*^{C118S/C118S} (C118S/C118S, 25 mice, 121 visible surface tumours) mice 8 months after treatment with urethane. Bars: mean ± s.e.m. NS: non-significant (P>0.05), **P<0.01 and ***P<0.001, as determined using one-way analysis of variance plus post-hoc Bonferroni's multiple comparison test.

Mutational bias against the *Kras*^{C118S} allele. We next tested whether there was a bias of oncogenic mutations induced by urethane in either the native or C118S *Kras* allele in *Kras*^{+/C118S} mice. To this end, RNA was extracted from 65 lung tumours from 20 *Kras*^{+/C118S} mice treated with urethane. *Kras* mRNA was then RT-PCR amplified, cloned and sequenced to identify the allelic origin (native or C118S) and mutation status (wild-type or

oncogenic). No oncogenic mutation was detected in either *Kras* allele in 21 tumours, only one allele was recovered in another 9 tumours and a mutation was detected in both alleles in 3 tumours. As such, these samples were excluded from the analysis. Of the remaining 32 tumours (derived from 15 *Kras*^{C118S/+} mice) in which both *Kras* alleles were recovered and there was an oncogenic mutation in only one of the alleles, 20 tumours had an

Table 2 | Quantification of surface lung tumours from urethane-treated mice.

Kras genotype	Number of mice	Tumour incidence (%)	Mean \pm s.e.m. tumours per lung	Total number of tumours	Tumour incidence by size (mm)		
					≤ 1 (%)	1-3 (%)	≥ 3 (%)
+/+	27	96.3	10.52 \pm 1.46	285	37.5	58.9	3.5
+/C118S	25	96.0	5.36 \pm 0.56	132	41.7	57.6	0.76
C118S/C118S	25	88.0	4.84 \pm 0.95	121	56.2	43.0	0.83

Table 3 | Histological quantification of lung adenomas from urethane-treated mice.

Kras genotype	Number of lung sections	Adenoma incidence (%)	Mean \pm s.e.m. adenomas per section	Total number of adenomas	Adenoma incidence by size (mm)		
					≤ 1 (%)	1-3 (%)	≥ 3 (%)
+/+	27	85.2	2.52 \pm 0.35	68	52.9	41.2	5.9
+/C118S	25	80.0	1.92 \pm 0.26	48	87.5	12.5	0
C118S/C118S	25	80.0	1.64 \pm 0.38	41	80.5	19.5	0

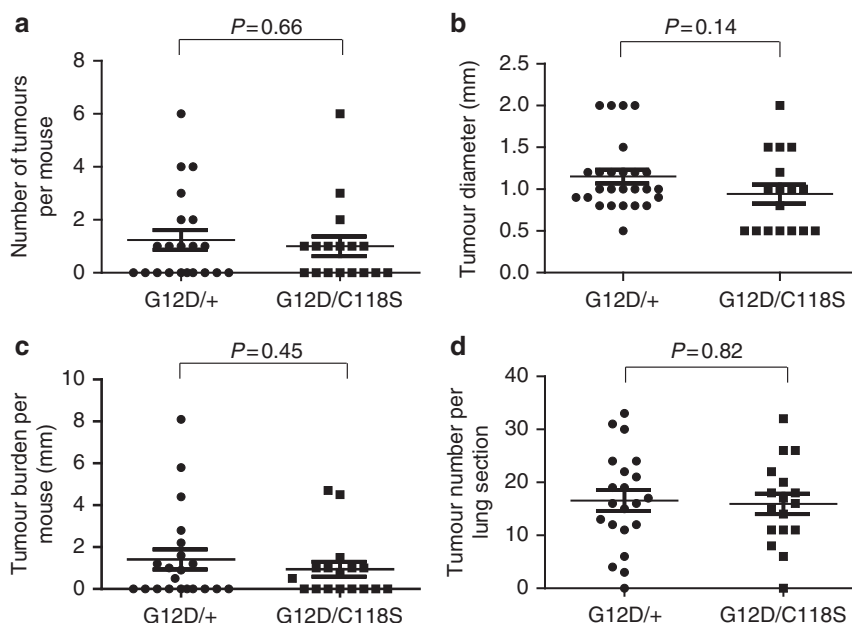


Figure 5 | *Kras*^{G12D}-driven lung tumorigenesis is similar when the remaining *Kras* allele is wild-type or C118S. (a) Number of visible surface tumour lesions per mouse, (b) diameter of each visible surface tumour lesion, (c) tumour burden, as defined by the sum of the diameters of all visible surface tumour lesions per mouse, and (d) number of lesions detected in each H&E-stained section from *Kras*^{LSL-G12D/+} (G12D/+, 21 mice, 26 visible surface tumours) versus *Kras*^{LSL-G12D/C118S} (G12D/C118S, 17 mice, 17 visible surface tumours) mice 4 months after intranasal administration of AdCre. Bars: mean \pm s.e.m. *P* values were determined using two-tailed unpaired Student's *t*-test.

oncogenic Q61R/L mutation in the native *Kras* allele, whereas 12 had the mutation in the *Kras*^{C118S} allele (Fig. 6 and Supplementary Table 3). This almost twofold enrichment in mutations recovered in the native *Kras* allele was significantly different from the expected frequency, assuming the incidence of oncogenic Q61R/L mutations occurring on the native *Kras* and the *Kras*^{C118S} allele was both 50% (χ^2 test, *P* = 0.0455).

The above results suggest a bias against oncogenic mutations in the *Kras*^{C118S} allele. Although preliminary experiments revealed that ectopic *Kras*^{Q61L,C118S} and *Kras*^{Q61L} behaved rather similarly with regards to signalling, transformation and oncogene-induced growth arrest, there did appear to be a potential consequence of mutating C118 in the G13D oncogenic mutant background. Specifically, *Kras*^{C118S/C118S} MEFs immortalized with the SV40 early region and transformed with either *Kras*^{G13D,C118S} or

Kras^{G13D} were treated with epidermal growth factor (EGF) to stimulate GEF activity, given the potential involvement of GEFs in activating oncogenic Ras proteins^{37,38}. Lysates derived three independent times from these two cell lines were then immunoblotted to detect ectopic *Kras*, endogenous tubulin, as well as total (T) and phosphorylated (P) Erk1/2. On average, this analysis revealed a trend towards a lower normalized P-Erk1/2 level upon EGF treatment in the *Kras*^{G13D,C118S} compared with *Kras*^{G13D}-transformed MEFs (Fig. 7a,b and Supplementary Fig. 6e). To exclude an involvement of wild-type *Hras* and *Nras* isoforms^{20,39}, the *Kras*^{C118S/C118S} genotype was crossed into an *Hras*^{-/-}; *Nras*^{-/-} background to generate *Kras*^{C118S/C118S}; *Hras*^{-/-}; *Nras*^{-/-} MEFs, which were then immortalized with the SV40 early region and transformed with either *Kras*^{G13D,C118S} or *Kras*^{G13D}. Based on three independent experiments, on

average there was a decrease in the normalized P-Erk1/2 levels upon EGF treatment in the $Kras^{G13D,C118S}$ compared with the $Kras^{G13D}$ -transformed $Kras^{C118S/C118S};Hras^{-/-};Nras^{-/-}$ MEFs (Fig. 7c,d and Supplementary Fig. 6f).

Discussion

We report that mutating C118 of endogenous *Kras* to serine suppressed urethane-induced lung tumorigenesis. We recognize that it is formally possible that the recombined *loxP* sites

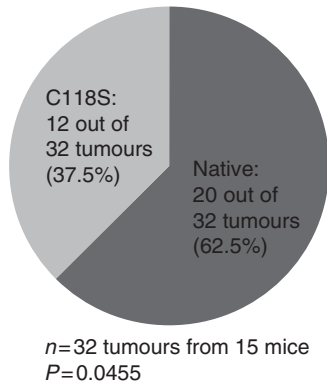


Figure 6 | Oncogenic Q61 mutations occur preferentially on the native *Kras* allele. Pie chart of the number and percent of Q61R/L oncogenic mutations found in the native versus the C118S *Kras* allele, as determined by RT-PCR amplification and sequencing of *Kras* mRNA isolated from 32 lung lesions from 15 $Kras^{+/C118S}$ mice 8 months after treatment with urethane. *P* value was determined using the χ^2 test to compare the difference between the observed and the expected frequency.

introduced into the intron during the generation of the $Kras^{C118S}$ allele could underlie this effect rather than the C118S mutation. However, such a possibility seems less likely given that the $Kras^{C118S}$ allele yielded both *Kras* 4A and *Kras* 4B transcripts, produced similar levels of protein compared with the native *Kras* allele, and had no observable phenotype in a homozygous setting. The C118S mutation also inhibits the ability of Ras proteins to be activated in the presence of reactive nitrogen or oxygen species^{6,8,10,12,17,18,22-24}. Thus, prior research additionally supports a plausible correlation between the mutation of the redox-reactive moiety at the C118 site and the observed reduction in tumorigenicity in mice with one or two $Kras^{C118S}$ alleles.

Introducing the C118S mutation into the remaining *Kras* allele in the $LSL-Kras^{G12D}$ model of lung cancer had no obvious effect on the number or size of resultant tumours, suggesting that the C118S mutation does not confer any overt change to the tumour-suppressive activity of the non-oncogenic allele. This does not, however, exclude a role for the C118 in the wild-type *Kras* protein in other settings. Indeed, the C118S mutation in wild-type *Hras* and *Nras* inhibits the xenograft tumour growth of some cancer cell lines²⁰. As such, the effect of mutating this residue may be temporal or context-dependent in cancer, consistent with the highly variable effects of, for example, nitric oxide on tumorigenesis⁴⁰. Nevertheless, extrapolating the results from this experiment, we suggest that the reduction of lung tumours in urethane-treated $Kras^{C118S/+}$ or $Kras^{C118S/C118S}$ mice may be more related to the oncogenic, rather than remaining non-oncogenic *Kras* allele.

Sequencing analysis suggests a preference of oncogenic mutations in the native compared with the C118S allele in tumours from $Kras^{+/C118S}$ mice treated with urethane. It is formally possible that carcinogens cause fewer mutations in the

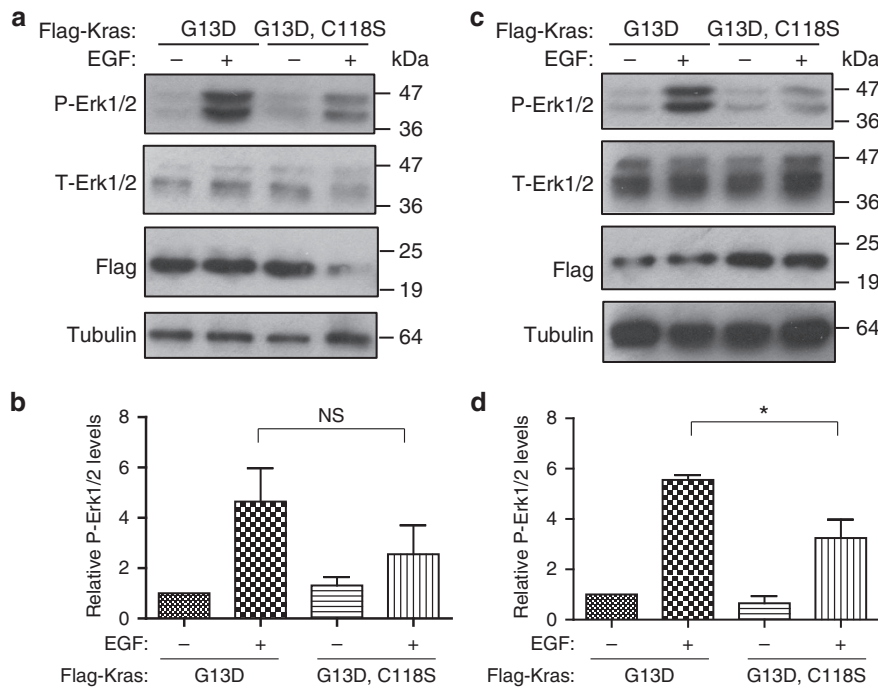


Figure 7 | Reduced increase in P-Erk1/2 levels in MEFs transformed with $Kras^{G13D,C118S}$ upon EGF treatment. Immunoblot of Flag-tagged ectopic *Kras*, tubulin, as well as total (T) and phosphorylated (P) Erk1/2 from (a) $Kras^{C118S/C118S}$ or (c) $Nras^{-/-};Hras^{-/-};Kras^{C118S/C118S}$ MEFs immortalized with the SV40 early region and transformed with either Flag- $Kras^{G13D}$ or Flag- $Kras^{G13D,C118S}$ in the absence or presence of EGF stimulation. (b,d) Mean \pm s.e.m. of P-Erk1/2 levels (normalized to T-Erk1/2) from three independent experiments using lysates from (b) $Kras^{C118S/C118S}$ or (d) $Nras^{-/-};Hras^{-/-};Kras^{C118S/C118S}$ MEFs immortalized with the SV40 early region and transformed with either Flag- $Kras^{G13D}$ or Flag- $Kras^{G13D,C118S}$ in the absence or presence of EGF stimulation. NS: non-significant ($P > 0.05$). * $P < 0.05$, as determined using one-way analysis of variance plus *post-hoc* Bonferroni's multiple comparison test.

Kras^{C118S} allele by some unknown mechanism. However, the C118S is only a point mutation, lies more than 2 kb away and in a completely different exon from where the Q61 oncogenic mutations occur, and is well established to block redox-dependent activation of Ras^{6,8,10,12,17,18,22–24}. Thus, we favour a model whereby an oncogenic mutation in the *Kras*^{C118S} allele is less likely to lead to productive tumorigenesis. Accumulating evidence suggests a potential role of GEFs in activating oncogenic Ras proteins^{37,38}, and in this regard, there was a difference in the ability of EGF to stimulate the MAPK pathway in cells transformed by *Kras*^{G13D,C118S} versus *Kras*^{G13D}. However, the relationship of NO and urethane tumorigenesis is undoubtedly more complex. NO can be generated from urethane derivatives in the appropriate conditions *in vitro*⁴¹ and *iNOS* knockout mice are resistant to this carcinogen⁴². As such, the apparent preference of oncogenic mutations in the native compared with the C118S allele of *Kras* awaits a biochemical or cellular explanation. In summary, these results indicate that urethane carcinogenesis is reduced in mice with the *Kras*^{C118S} allele, an effect that may be linked to the oncogenic rather than the native *Kras* version of the gene.

Methods

Plasmids. pBabeNeo-SV40-T-t-Ag (encoding the early region of SV40) was described previously^{20,43}. pBabeBleo-eNOS^{S1177D}-HA was generated by introducing a mutation resulting in a S1177D amino-acid change into C-terminal HA-epitope-tagged eNOS cDNA²⁰. pBabePuroFlag-Kras^{G13D} was generated by introducing a mutation resulting in a G13D amino-acid change into N-terminal FLAG-epitope-tagged human *Kras* cDNA²⁰. pBabePuroFlag-Kras^{G13D,C118S} was generated by introducing a mutation resulting in a C118S amino-acid change into the aforementioned pBabePuroFlag-Kras^{G13D} plasmid.

Animals. All animal experiments were approved by an Institutional Animal Care and Use Committee at Duke University. 129S6/SvEvTac mice were from Taconic. C57BL/6 mice (C57BL/6N), CMVCre transgenic mice (B6.C-Tg (CMV-cre) 1Cgn/J) and *Kras*^{LSL-G12D} transgenic mice (129S/Sv-Kras^{tm4Tyj}/J) were obtained from Jackson Laboratory. *Kras*^{C118S} knock-in mice were generated at Transgenic Mouse Facility of Duke Cancer Institute. The described targeting vector (Fig. 1a) was linearized with *NotI* and electroporated into W4 ES cells from 129S6/SvEvTac mice, followed by positive selection with G418 and negative selection with ganciclovir. RNA was isolated from individual ES cell clones, and RT-PCR was performed with primers P1 and P2 to amplify *Kras* cDNA (Supplementary Table 4). PCR products were resolved in 2% agarose gels, purified by a gel purification kit (Qiagen), and sequenced to confirm the *Kras*^{C118S} mutation. One successfully targeted clone was injected into C57BL/6 blastocysts, which were then implanted into pseudo-pregnant females to generate chimeras. Male chimeras were bred with female C57BL/6 mice, and offspring with germline transmission of the *Kras*^{C118S(Neo)} allele were identified by PCR of genomic DNA with primer pairs P3 + P4 specific for the *Kras*^{C118S} allele and P3 + P5 specific for the wild-type allele (Supplementary Table 4) as well as direct sequencing of *Kras* RT-PCR products from lung tissue. Male *Kras*^{+ / C118S(Neo)} mice were bred with female CMVCre transgenic mice to excise the *Neo* cassette. The genotypes of offspring were identified by PCR of genomic DNA using the primer pair P3 + P5 to identify the wild-type *Kras* allele and the *Kras*^{C118S} allele lacking the *Neo* cassette. Absence of the *Neo* cassette was also confirmed with primer pair P3 + P4, which does not generate a product when the *Neo* cassette is deleted. CMVCre;*Kras*^{+ / C118S} mice were then crossed with *Kras*^{+ / +} mice to generate *Kras*^{+ / C118S} mice without CMVCre for use in all the animal studies. *Kras*^{+ / C118S} mice were crossed to generate *Kras*^{+ / +}, *Kras*^{+ / C118S} and *Kras*^{C118S / C118S} mice, whose genotypes were again identified by PCR of genomic DNA using the primer pair P3 + P5. *Kras*^{+ / C118S} mice were further crossed into *Nras*^{- / -}; *Hras*^{- / -} background to generate *Nras*^{- / -}; *Hras*^{- / -}; *Kras*^{+ / C118S} mice.

Generation of MEFs and cell culture. All the cells were maintained in Dulbecco's modified Eagle's medium (DMEM) supplemented with 10% fetal bovine serum (FBS) and incubated at 37 °C in a 5% CO₂ incubator. *Kras*^{+ / +} and *Kras*^{C118S / C118S} MEFs were prepared from embryos from *Kras*^{C118S / +} females bred with a *Kras*^{C118S / +} male. Embryos (E13-E16) were dissected from euthanized pregnant *Kras*^{C118S / +} females and washed with sterile PBS. The head of each embryo was removed for isolation of genomic DNA and identification of genotypes by PCR using primers P3 + P5 as described above. The remaining embryos were cut into pieces in a sterile dish and incubated with 1 ml 0.25% trypsin at 37 °C in a 5% CO₂ incubator for 30–45 min. The trypsinized cells were then mixed with 10 ml 10% FBS DMEM and incubated at 37 °C in a 5% CO₂ incubator for further experiments.

Nras^{- / -}; *Hras*^{- / -}; *Kras*^{C118S / C118S} MEFs were prepared as above from embryos from an *Nras*^{- / -}; *Hras*^{- / -}; *Kras*^{C118S / +} female bred with an *Nras*^{- / -}; *Hras*^{- / -}; *Kras*^{C118S / +} male. Primary MEF lines were immortalized by stable infection⁴³ with retroviruses derived from pBabeNeo-SV40-T-t-Ag. In some cases these cells were further stably infected⁴³ with retroviruses derived from pBabeBleo, pBabeBleo-eNOS^{S1177D}-HA, pBabePuroFlag-Kras^{G13D} or pBabePuroFlag-Kras^{G13D,C118S}. Where indicated, immortalized MEFs were serum starved by incubating with 0.5% FBS DMEM overnight and harvested the next day. Where indicated, immortalized MEFs were also treated with 100 ng μl⁻¹ EGF (Sigma) for 5 min at 37 °C in a 5% CO₂ incubator before being harvested on ice.

Immunoblot analysis. Cells or lung tissue were lysed with RIPA buffer (1% NP-40, 20 mM Tris, pH 8.0, 137 mM NaCl, 10% glycerol, 2mM EDTA) and protein concentrations quantified by Bradford assay (Bio-Rad). Equal amounts of protein lysates (50 μg) were resolved by SDS-polyacrylamide gel electrophoresis, transferred to a polyvinylidene difluoride membrane and immunoblotted with primary antibodies: anti-Kras F234 (Santa Cruz, sc-30, diluted 1:200), anti-Flag M2 (Sigma, F1804, diluted 1:500), anti-HA (Covance, diluted 1:1,000), anti-β-actin (Sigma, A2228, diluted 1:10,000), anti-β-tubulin (Sigma, T5201, diluted 1:2,000), anti-Erk1/2 (Santa Cruz, sc-94, diluted 1:2,000) or anti-P (Thr 202/Tyr 204)-Erk1/2 (Santa Cruz, sc-7383, diluted 1:500), followed by incubation with either goat anti-rabbit (Santa Cruz, sc-2004, diluted 1:5,000) or anti-mouse (Invitrogen, G21040, diluted 1:10,000) IgG-HRP-conjugated secondary antibodies and detected by ECL (GE Healthcare). Bands of targeted protein in scanned images were quantified using Image J software and normalized.

RT-PCR. RNA was extracted from ES cells, lung tissue or lung tumours with the RNA-BEE reagent according to the manufacturer's protocol (Fisher Scientific). 0.5–2 μg of RNA was reverse transcribed using Omniscript RT kit (Qiagen) and Oligo dT (Qiagen) as primers. Resultant cDNA was used as a template to amplify targets of interest using the primers listed in Supplementary Table 4.

Urethane carcinogenesis. *Kras*^{+ / C118S} mice (without CMVCre) were bred with *Kras*^{+ / +} mice in 129S6/SvEvTac background. Resultant *Kras*^{+ / C118S} mice were then crossed to generate *Kras*^{+ / +}, *Kras*^{+ / C118S} and *Kras*^{C118S / C118S} littermates in which both *Kras* alleles originated from a 129S6/SvEvTac background. Twenty-five to twenty-seven male and female mice of each genotype were ultimately compared with detect a measurable difference in tumour parameters between control and experimental cohorts. A total of 38 male and 39 female mice at 2 months of age were intraperitoneally injected with urethane (1 mg g⁻¹ body weight)³⁵. Weight and behaviour were monitored twice weekly starting at 3 months post injection. Eight months after injection, mice were euthanized, and lungs were inflated with PBS and harvested for analysis. Lung surface tumours were counted under a dissecting microscope. Tumour diameter was determined using micro-calipers. Mice that reached moribundity end points before 8 months were excluded from the final analysis. The investigator was blinded to the genotype when injecting urethane as well as when assessing tumour number and size.

Ad-Cre-induced lung tumorigenesis. *Kras*^{+ / C118S} mice in which both *Kras* alleles originated from a 129S6/SvEvTac background were bred with *LSL-Kras*^{G12D / +} mice to generate *Kras*^{LSL-G12D / +} and *Kras*^{LSL-G12D / C118S} mice. Seventeen to twenty-one male and female mice of each genotype were ultimately compared to detect a measurable difference in tumour parameters between control and experimental cohorts. Nine male and twenty-nine female mice were infected with 6 × 10⁶ p.f.u. of AdCre virus at 2 months of age³⁶. Weight and behaviour were monitored twice weekly starting at 3 months post-AdCre. Four months after AdCre administration, mice were euthanized and lungs were inflated with PBS and harvested for analysis. Surface tumours were counted under a dissecting microscope. Tumour diameter was determined using micro-calipers. Mice that reached moribundity end points before 4 months were excluded from the final analysis. The investigator was blinded to the genotype when administering AdCre as well as when assessing tumour number and size.

Histological analysis. Left lobes of lungs from the indicated mice (see above) were fixed in 10% neutral buffered formalin overnight, dehydrated in 70% ethanol and paraffin embedded. 5 μm-thick sections were cut from each sample, mounted on glass slides and stained with H&E. A total of 77 lung sections were reviewed by two pathologists (D.M.C. and J.C.) who were masked to the study design and blinded to the genotype. The number and type (AAH, AD and/or AC) of lesions were quantified in each sample. Adenomas were further classified by size (≤ 1, 1–3 or ≥ 3 mm) and histological subtype (solid, papillary or mixed solid-papillary)³⁴.

Immunohistochemistry. Left lobes of lungs from the indicated mice (see above) were fixed in 10% neutral buffered formalin overnight, dehydrated in 70% ethanol and paraffin embedded. 5 μm-thick sections were cut from each sample, mounted on glass slides and subjected to epitope retrieval and stained with anti-P(Thr

202/Tyr 204)-Erk1/2 (Cell Signaling, 4376), anti-P(Ser473)-Akt (Cell Signaling, 4060) or anti-Ki67 (Thermo Scientific, RM9106) antibodies followed by peroxidase-based detection with Vectastain Elite ABC Kits (Vector Labs) and counterstained with haematoxylin. Photographs were taken of four to six high-power ($\times 20$) random fields with tumour areas on an Olympus Vanox S microscope (Olympus). Images were blinded and tumours were circumscribed in stained tissue images with the freehand selection tool in Image J, and the total area of the tumour in pixels was recorded. Tumour images were copied and pasted to new, blank images and colour threshold was applied to determine positive-staining areas, using the same parameters for each tumour image. Areas staining positive by these parameters were selected and the positive staining area in pixels was recorded. The percentage of positive-staining area was calculated by dividing the positive-staining area of the tumour in pixels by the total area of tumours in pixels.

Kras mutation analysis. Lung tumours arising in urethane-treated *Kras*^{+/*C118S*} mice (see above) were removed with the aid of a dissection microscope. A measure of 500 ng of RNA isolated from the tumours were RT-PCR amplified (see above) using the primer pair P6 + P7 containing *Hind*III and *Sac*I sites, respectively (Supplementary Table 4). Resultant products were cloned into the *Hind*III and *Sac*I sites of pBluescript vector (from Addgene), after which 12 positive clones from each ligation reaction were sequenced using T7 promoter (Eton Bioscience) to determine whether the clone corresponded to the native or C118S allele of *Kras*, and whether the clone had an oncogenic mutation (at position G12, G13 and Q61).

Statistical analysis. Data were presented as mean values \pm standard error of the mean (s.e.m.). Most statistical analyses were performed with Graphpad Prism 5 software. The two-tailed unpaired Student's *t*-test was used to compare two groups. The one-way analysis of variance plus *post-hoc* Bonferroni's multiple comparison tests were used to compare three or more groups. The multivariate analysis of variance test was used to compare mice weight change over time between two groups, whereas the long-rank test was performed to compare the survival between two groups. The χ^2 test was used to analyse difference in frequency (between the observed versus the expected or between two groups) based on contingency tables. *P* values <0.05 were considered significant.

References

- Pylayeva-Gupta, Y., Grabocka, E. & Bar-Sagi, D. RAS oncogenes: weaving a tumorigenic web. *Nat. Rev. Cancer* **11**, 761–774 (2011).
- Downward, J. Targeting RAS signalling pathways in cancer therapy. *Nat. Rev. Cancer* **3**, 11–22 (2003).
- Gysin, S., Salt, M., Young, A. & McCormick, F. Therapeutic strategies for targeting ras proteins. *Genes Cancer* **2**, 359–372 (2011).
- Bos, J. L., Rehmann, H. & Wittinghofer, A. GEFs and GAPs: critical elements in the control of small G proteins. *Cell* **129**, 865–877 (2007).
- Vigil, D., Cherfils, J., Rossman, K. L. & Der, C. J. Ras superfamily GEFs and GAPs: validated and tractable targets for cancer therapy? *Nat. Rev. Cancer* **10**, 842–857 (2010).
- Lander, H. M. *et al.* Redox regulation of cell signalling. *Nature* **381**, 380–381 (1996).
- Raines, K. W., Bonini, M. G. & Campbell, S. L. Nitric oxide cell signaling: S-nitrosylation of Ras superfamily GTPases. *Cardiovas. Res.* **75**, 229–239 (2007).
- Hobbs, G. A., Bonini, M. G., Gunawardena, H. P., Chen, X. & Campbell, S. L. Glutathiolated Ras: characterization and implications for Ras activation. *Free Radic. Biol. Med.* **57**, 221–229 (2013).
- Ibiza, S. *et al.* Endothelial nitric oxide synthase regulates N-Ras activation on the Golgi complex of antigen-stimulated T cells. *Proc. Natl. Acad. Sci. USA* **105**, 10507–10512 (2008).
- Lander, H. M. *et al.* A molecular redox switch on p21(ras). Structural basis for the nitric oxide-p21(ras) interaction. *J. Biol. Chem.* **272**, 4323–4326 (1997).
- Lander, H. M., Jacovina, A. T., Davis, R. J. & Tauras, J. M. Differential activation of mitogen-activated protein kinases by nitric oxide-related species. *J. Biol. Chem.* **271**, 19705–19709 (1996).
- Raines, K. W., Cao, G. L., Lee, E. K., Rosen, G. M. & Shapiro, P. Neuronal nitric oxide synthase-induced S-nitrosylation of H-Ras inhibits calcium ionophore-mediated extracellular-signal-regulated kinase activity. *Biochem. J.* **397**, 329–336 (2006).
- Switzer, C. H. *et al.* Ets-1 is a transcriptional mediator of oncogenic nitric oxide signaling in estrogen receptor-negative breast cancer. *Breast Cancer Res.* **14**, R125 (2012).
- Lin, Y. F., Raab-Graham, K., Jan, Y. N. & Jan, L. Y. NO stimulation of ATP-sensitive potassium channels: Involvement of Ras/mitogen-activated protein kinase pathway and contribution to neuroprotection. *Proc. Natl. Acad. Sci. USA* **101**, 7799–7804 (2004).
- Lee, M. & Choy, J. C. Positive feedback regulation of human inducible nitric-oxide synthase expression by Ras protein S-nitrosylation. *J. Biol. Chem.* **288**, 15677–15686 (2013).
- Batista, W. *et al.* S-Nitrosoglutathione and endothelial nitric oxide synthase-derived nitric oxide regulate compartmentalized ras S-nitrosylation and stimulate cell proliferation. *Antioxid. Redox Signal.* **18**, 221–238 (2013).
- Adachi, T. *et al.* S-Glutathiolation of Ras mediates redox-sensitive signaling by angiotensin II in vascular smooth muscle cells. *J. Biol. Chem.* **279**, 29857–29862 (2004).
- Clavreul, N. *et al.* S-Glutathiolation by peroxynitrite of p21ras at cysteine-118 mediates its direct activation and downstream signaling in endothelial cells. *FASEB J.* **20**, 518–520 (2006).
- Dudzinski, D. M., Igarashi, J., Greif, D. & Michel, T. The regulation and pharmacology of endothelial nitric oxide synthase. *Annu. Rev. Pharmacol. Toxicol.* **46**, 235–276 (2006).
- Lim, K. H., Ancrile, B. B., Kashatus, D. F. & Counter, C. M. Tumour maintenance is mediated by eNOS. *Nature* **452**, 646–649 (2008).
- Sarkisian, C. J. *et al.* Dose-dependent oncogene-induced senescence in vivo and its evasion during mammary tumorigenesis. *Nat. Cell Biol.* **9**, 493–505 (2007).
- Heo, J. & Campbell, S. L. Mechanism of p21Ras S-nitrosylation and kinetics of nitric oxide-mediated guanine nucleotide exchange. *Biochemistry* **43**, 2314–2322 (2004).
- Mott, H. R., Carpenter, J. W. & Campbell, S. L. Structural and functional analysis of a mutant Ras protein that is insensitive to nitric oxide activation. *Biochemistry* **36**, 3640–3644 (1997).
- Williams, J. G., Pappu, K. & Campbell, S. L. Structural and biochemical studies of p21Ras S-nitrosylation and nitric oxide-mediated guanine nucleotide exchange. *Proc. Natl. Acad. Sci. USA* **100**, 6376–6381 (2003).
- Patek, C. E. *et al.* Mutationally activated K-ras 4A and 4B both mediate lung carcinogenesis. *Exp. Cell Res.* **314**, 1105–1114 (2008).
- To, M. D. *et al.* Kras regulatory elements and exon 4A determine mutation specificity in lung cancer. *Nat. Genet.* **40**, 1240–1244 (2008).
- Dimmeler, S. *et al.* Activation of nitric oxide synthase in endothelial cells by Akt-dependent phosphorylation. *Nature* **399**, 601–605 (1999).
- Fulton, D. *et al.* Regulation of endothelium-derived nitric oxide production by the protein kinase Akt. *Nature* **399**, 597–601 (1999).
- Koera, K. *et al.* K-ras is essential for the development of the mouse embryo. *Oncogene* **15**, 1151–1159 (1997).
- You, M., Candrian, U., Maronpot, R. R., Stoner, G. D. & Anderson, M. W. Activation of the Ki-ras protooncogene in spontaneously occurring and chemically induced lung tumors of the strain A mouse. *Proc. Natl. Acad. Sci. USA* **86**, 3070–3074 (1989).
- Ding, L. *et al.* Somatic mutations affect key pathways in lung adenocarcinoma. *Nature* **455**, 1069–1075 (2008).
- Manenti, G. *et al.* Haplotype sharing suggests that a genomic segment containing six genes accounts for the pulmonary adenoma susceptibility 1 (Pas1) locus activity in mice. *Oncogene* **23**, 4495–4504 (2004).
- Stathopoulos, G. T. *et al.* Epithelial NF-kappaB activation promotes urethane-induced lung carcinogenesis. *Proc. Natl. Acad. Sci. USA* **104**, 18514–18519 (2007).
- Avanzo, J. L. *et al.* Increased susceptibility to urethane-induced lung tumors in mice with decreased expression of connexin43. *Carcinogenesis* **25**, 1973–1982 (2004).
- Zhang, Z. *et al.* Wildtype Kras2 can inhibit lung carcinogenesis in mice. *Nat. Genet.* **29**, 25–33 (2001).
- Jackson, E. L. *et al.* Analysis of lung tumor initiation and progression using conditional expression of oncogenic K-ras. *Genes Dev.* **15**, 3243–3248 (2001).
- Hocker, H. J. *et al.* Andrographolide derivatives inhibit guanine nucleotide exchange and abrogate oncogenic Ras function. *Proc. Natl. Acad. Sci. USA* **110**, 10201–10206 (2013).
- Huang, H. *et al.* Oncogenic K-Ras requires activation for enhanced activity. *Oncogene* **33**, 532–535 (2014).
- Jeng, H. H., Taylor, L. J. & Bar-Sagi, D. Sos-mediated cross-activation of wild-type Ras by oncogenic Ras is essential for tumorigenesis. *Nat. Commun.* **3**, 1168 (2012).
- Fukumura, D., Kashiwagi, S. & Jain, R. K. The role of nitric oxide in tumour progression. *Nat. Rev. Cancer* **6**, 521–534 (2006).
- Sakano, K., Oikawa, S., Hiraku, Y. & Kawanishi, S. Metabolism of carcinogenic urethane to nitric oxide is involved in oxidative DNA damage. *Free Radic. Biol. Med.* **33**, 703–714 (2002).
- Kisley, L. R. *et al.* Genetic ablation of inducible nitric oxide synthase decreases mouse lung tumorigenesis. *Cancer Res.* **62**, 6850–6856 (2002).
- O'Hayer, K. M. & Counter, C. M. A genetically defined normal human somatic cell system to study ras oncogenesis in vivo and in vitro. *Methods Enzymol.* **407**, 637–647 (2006).

Acknowledgements

We thank the Duke Cancer Institute Mouse Transgenic Facility for aid in generating mice with a *Kras*^{C118S} allele, Benjamin Lampson for assistance in the design of the targeting vector, Nicole Pershing for technical assistance with lung tumour models, Jianqi Zhang for assistance with statistical analysis, and Sharon Campbell, Aaron Hobbs,

Donita Brady and Matt Crowe for review of the manuscript and/or reagents. This work is supported by NIH grant CA123031 (C.M.C.).

Author contributions

L.H. and C.M.C. conceived the study. L.H. performed the experiments. D.M.C. and J.C. performed histological analysis of lung tumours. All authors contributed to the writing of the manuscript.

Additional information

Competing financial interests: The authors declare no competing financial interests.

Reprints and permission information is available online at <http://npg.nature.com/reprintsandpermissions/>

How to cite this article: Huang, L. *et al.* Decreased tumorigenesis in mice with a *Kras* point mutation at C118. *Nat. Commun.* 5:5410 doi: 10.1038/ncomms6410 (2014).